



Cite this: *Chem. Commun.*, 2022,  
58, 1203

Received 1st November 2021,  
Accepted 21st December 2021

DOI: 10.1039/d1cc06121f

rsc.li/chemcomm

# Intercalation electrochemistry for thermoelectric energy harvesting from temperature fluctuations†

Christian Heubner,<sup>a</sup> Tobias Liebmann,<sup>b</sup> Michael Schneider<sup>a</sup> and  
Alexander Michaelis<sup>ab</sup>

**The effective use of energy from sustainable sources is considered a crucial step on the way to a CO<sub>2</sub>-neutral economy. Low-grade waste heat (<100 °C) is widely and ubiquitously available, but difficult to convert into electrical energy with current technologies. Here, we demonstrate an electrochemical cell capable of directly converting ambient temperature fluctuations into electricity. Based on intercalation reactions with different entropies, any temperature change leads to a cell voltage and electrical energy can be extracted. The new cell concept features the advantages of thermo-electrochemical cells and pyroelectric-like energy harvesting, which opens a wide range of possibilities for effective and sustainable use of low-grade waste heat.**

Sustainable energy generation is one of the central issues of our time and of crucial importance for the future of society. Low-grade waste heat (*i.e.*, with temperatures <100 °C), such as that generated by industrial or geothermal processes, is a particularly important source of energy that can be used to generate electricity.<sup>1,2</sup> In parallel, there is growing interest in portable electronic devices and autonomous systems that are self-sustaining through the harvesting of low-grade heat, such as that generated by the human body.<sup>3,4</sup>

Until recently, thermal energy conversion has been primarily studied in the field of solid-state thermoelectrics. Thermoelectric materials generate electrical energy from temperature gradients ( $dT/dx$ ) by exploiting the Seebeck effect. However, these devices have limited efficiency at temperatures <100 °C, making them unsuitable for low-grade heat harvesting.<sup>5</sup> Thermo-electrochemical cells, also called thermocells, are an alternative design that is showing increasing promise for low-grade thermal energy conversion.<sup>6</sup> However, the need for a T-gradient has some disadvantages. To maintain the T-gradient,

the electrodes must be as thermally isolated from each other as possible. At the same time, the electrical resistance between them must be as low as possible, which is an intrinsic compromise. Alternatively, pyroelectric materials convert temperature fluctuations ( $dT/dt$ ) into electrical energy,<sup>7,8</sup> which allows the use of naturally occurring temperature variations, such as ambient temperature (*e.g.*, day-night cycle). Pyroelectric materials are of interest because they can operate at high thermodynamic efficiency under the right conditions and do not require bulky heat sinks.<sup>9</sup> Even though the efficiency of pyroelectric energy harvesting at temperatures <100 °C is much higher than that of thermoelectrics, the mean power generated is typically low, *i.e.* 1  $\mu\text{W cm}^{-3}$ .<sup>10</sup>

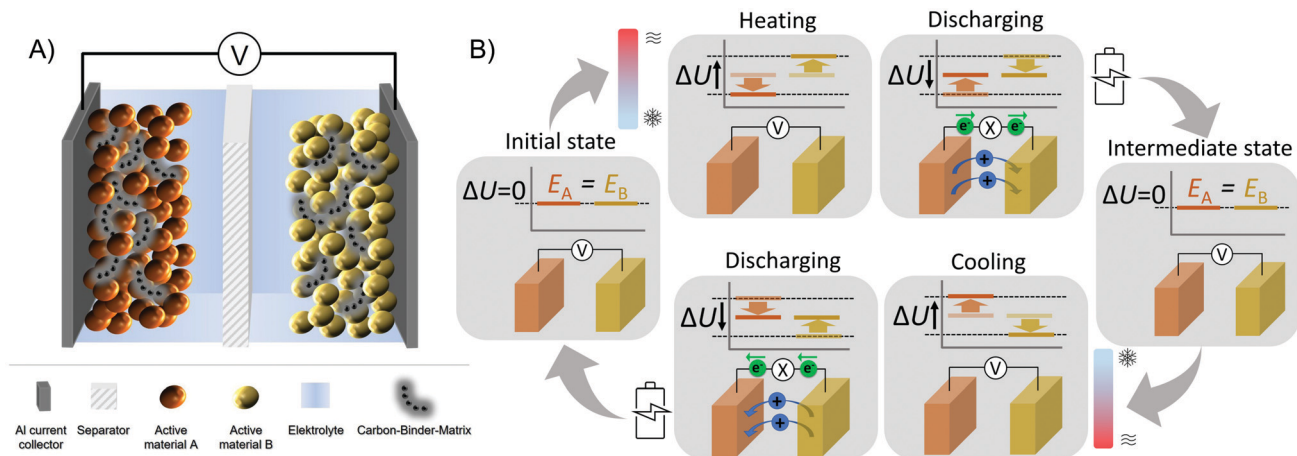
We conceived a novel type of electrochemical cell that features the advantages of pyroelectric-like behaviour and thermocells for harvesting of low-grade heat. It uses electrochemical reactions based on intercalation chemistry to convert thermal energy directly into electricity. The cell consists of two alkali-metal-ion intercalation electrodes separated by a porous membrane soaked with an electrolyte (Scheme 1A). In the initial state, the electrodes exhibit the same electrode potential, resulting in a cell voltage of 0 V (Scheme 1B). A change in temperature induces a drifting apart of the electrode potentials according to their individual temperature dependencies. Literally, the temperature change charges the cell. Subsequently, electric power can be drawn until the electrode potentials converge again and the cell voltage becomes zero. During this discharging process, ions are extracted from the electrode with lower potential and inserted into its counterpart. Returning to the initial temperature again induces a cell voltage and charging of the cell, respectively. In this case, discharging leads to the reverse of the previous ion shuttling between the electrodes. Consequently, periodic temperature changes can be used to continuously accumulate energy, *e.g.* charging of a battery. The development of intercalation chemistry in the early 1970s has enabled the use of novel and efficient electrode materials for electrochemical storage. A striking example are transition metal oxides, which can absorb and release alkali metal ions such as lithium and sodium through electrochemical reduction

<sup>a</sup> Fraunhofer IKTS, Fraunhofer Institute for Ceramic Technologies and Systems, Dresden, Germany. E-mail: christian.heubner@ikts.fraunhofer.de

<sup>b</sup> Institute of Materials Science, TU Dresden, Dresden, Germany

† Electronic supplementary information (ESI) available. See DOI: 10.1039/d1cc06121f





**Scheme 1** (A) Schematic drawing of cell construction including composite electrodes (intercalation materials, binder, conductive additive), separator and electrolyte. (B) Illustration of the working principle of electrochemical conversion of waste heat into electricity using intercalation chemistry. A temperature change causes the electrode potentials to drift apart according to their individual temperature dependence. Electrical energy can then be extracted from the cell until the electrode potentials converge. During the discharge process, intercalated ions are extracted from and inserted into the electrode with the lower and higher potential, respectively. Returning to the initial temperature causes the cell to charge again. In this case, energy extraction leads to the reversal of the previous ionic shuttling between the electrodes and return to the initial state again.

and oxidation of the host lattice.<sup>11</sup> First, we investigated materials known from Li-ion battery research. Porous composite electrodes based on  $\text{LiCoO}_2$  (LCO) and  $\text{LiNi}_{1/3}\text{Co}_{1/3}\text{Mn}_{1/3}\text{O}_2$  (NCM) were prepared and assembled in coin cells with  $\text{LiPF}_6$  based electrolyte (see ESI† for details).

As shown in Fig. 1a, the voltage ( $U$ ) of the NCM|LCO cell increases from 0 to 18 mV when increasing the temperature by

40 K, with NCM having the higher potential. The cell is then discharged at constant temperature and a current density of  $1 \mu\text{A cm}^{-2}$  until the cell voltage is reduced to 0 V again. An electric charge of  $25 \mu\text{A h cm}^{-2}$  is converted at an average voltage of 10 mV. This corresponds to a specific energy of about  $65 \mu\text{W h cm}^{-3}$  and an average power density of  $22 \mu\text{W cm}^{-3}$ , related to the volume,  $V$ , of the active materials. The conversion

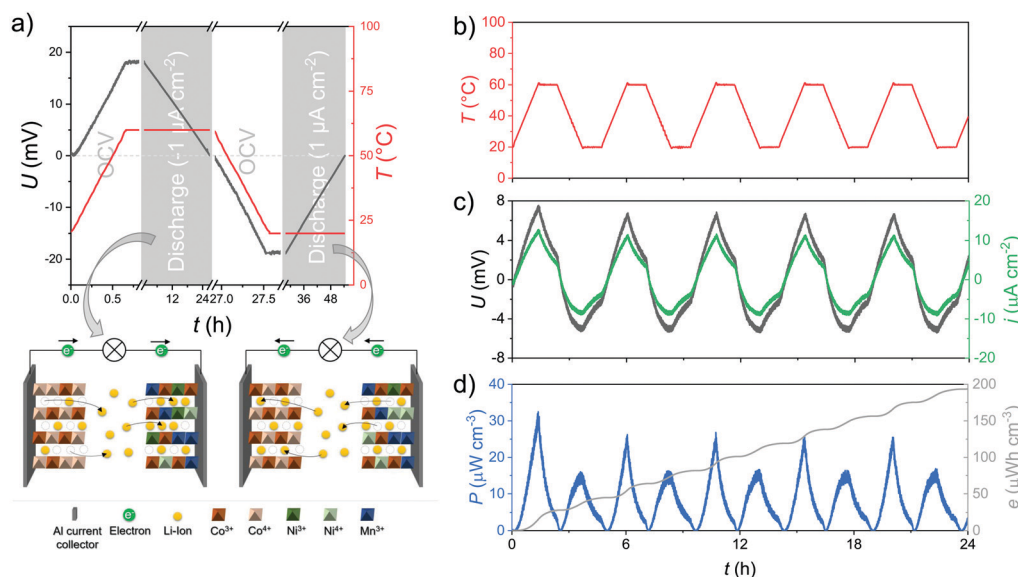


**Fig. 1** (a) Demonstration of thermal-electrical energy generation using intercalation chemistry using the example of a  $\text{Li}_{0.95}\text{CoO}_2$  |  $\text{Li}_{0.63}\text{Ni}_{1/3}\text{Co}_{1/3}\text{Mn}_{1/3}\text{O}_2$  cell: The increase in temperature leads to build-up of the cell voltage. During the subsequent constant current discharge, electrical energy is obtained by electrochemical reactions at the electrodes and the associated Li transfer (below) until the cell voltage has dropped to zero volts again. The subsequent reduction of the temperature leads again to the build-up of a cell voltage, allows the extraction of electrical energy by reversing the electrochemical reactions (below) and reaching the initial state again. Demonstration of continuous power generation from thermal fluctuations: (b) Temperature course, (c) Cell voltage and current density, and (d) Electrical power and energy extracted during continuous temperature changes between 20 and 60 °C.

efficiency, given by the ratio of electrical energy extracted  $\int IU dt$  and the thermal energy provided  $\int C dT$ , where  $C$  is the heat capacity of the active materials, is determined to 1.4% with respect to the Carnot limit. Note that the achieved power parameters are reduced when considering the cell level as described in the ESI† During this discharging process,  $\text{Co}^{3+}$  in LCO is oxidized to  $\text{Co}^{4+}$  and a corresponding number of Li-ions are removed from the host lattice.<sup>12</sup> At the same time,  $\text{Ni}^{4+}$  in the NCM host lattice is electrochemically reduced to  $\text{Ni}^{3+}$  and Li-ions are taken up from the electrolyte for charge compensation.<sup>13</sup> The insertion and extraction of Li-ions affects the equilibrium potential of NCM and LCO. When the equilibrium potentials are converged, the cell voltage is zero and the discharge reaction stops.

If the system is then returned to the initial temperature, a cell voltage builds up again, this time with a negative sign. In this case, LCO has the higher potential. During discharge,  $\text{Co}^{4+}$  in LCO is now reduced to  $\text{Co}^{3+}$  and the NCM host lattice is oxidized. Accordingly, Li-ions migrate from NCM to LCO until the equilibrium potentials of the materials equalize. Note that in both cases, positive as well as negative deflection of the voltage, energy can be extracted from the system, since the currents have the opposite sign in each case and thus always result in a net profit.

To investigate the reversibility of the processes, an electrical resistor (465  $\Omega$ ) was used as a model consumer and the temperature was periodically varied between 20–60 °C. This approach leads to reproducible cycles of voltage build-up and electrical discharge across the resistor (Fig. 1c). A slight

asymmetry of the discharge process at high and low temperatures is observed, which can be explained by different limitations of the intercalation kinetics. At low temperatures, charge transfer and Li-ion transport are more inhibited,<sup>14</sup> resulting in lower current density for the same voltage difference. This is also evident in Fig. 1d where the maximum power during heating is larger than for cooling. Despite this asymmetry, the cell can be operated in a reversible manner. A maximum power of about 33  $\mu\text{W cm}^{-3}$  is achieved and energy is accumulated continuously from the temperature fluctuations, *i.e.*  $\sim 200 \mu\text{W h cm}^{-3}$  from 5 cycles between 20–60 °C. In total, we operated the cell for 3 weeks at relatively slow temperature cycles (0.5 K  $\text{min}^{-1}$ ). An electrical energy of  $\sim 3 \text{ mWh cm}^{-3}$  was accumulated and no degradation of the performance could be detected (see ESI†). These power parameters may already be sufficient for some autonomous systems, *e.g.* wireless sensor networks, whose typical power requirements are in the  $\mu\text{W}$  to  $\text{mW}$  range.

The mechanism for the conversion of thermal to electrical energy is shown in Fig. 2a. A change in temperature causes a shift in the potential corresponding to the entropy of Li-intercalation,  $\Delta_R S$ . If the entropies of the electrode reactions are different, a cell voltage is formed. During discharge by the exchange of Li-ions between the electrodes, electric charge is converted according to the redox reactions taking place. The amount of electric charge is proportional to the differential capacity,  $dQ/dE$ . The smaller the potential change  $dE$  of the electrodes per transferred Li-ion, the greater the amount of electrical charge  $dQ$  that can be extracted until the electrode potentials converge. This way the cell mimics a thermodynamic

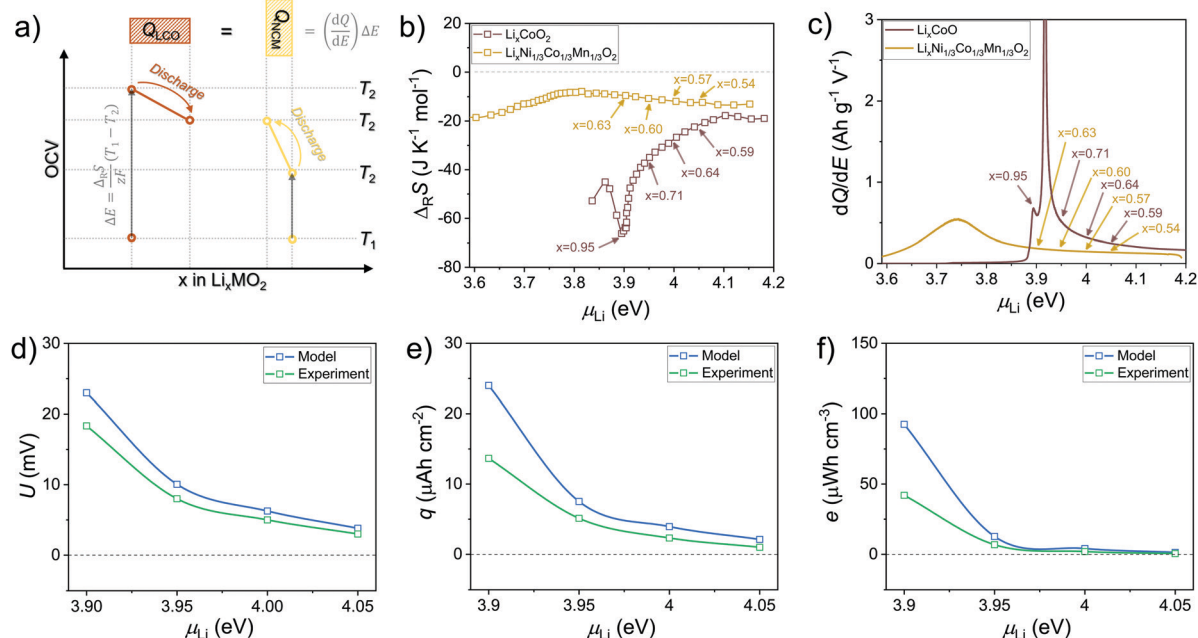


**Fig. 2** (a) Model description of electrochemical conversion of waste heat into electricity using the example of an LCO/NCM cell ( $z$  – valence (1),  $F$  – Faraday constant (96.485 As  $\text{mol}^{-1}$ )). (b) Entropy and (c) differential capacity of Li-ion intercalation in LCO and NCM. Comparison of model predictions and experimental results regarding (d) open circuit voltage, (e) electrical charge converted and (f) electrical energy extracted by changing the temperature from 20 to 60 °C.

heat engine. The specific electric charge is analogous to the volume, and the voltage is analogous to the pressure of the working fluid. The corresponding thermodynamic cycle corresponds most closely to an electrical Ericsson (Olsen) cycle.<sup>15</sup>

For the theoretical quantification of the thermal-electrical conversion effect illustrated in Fig. 2a, we made use of fundamental relationships based on equilibrium thermodynamics described in detail in the ESI.†

$$e = \frac{1}{2z^2 F^2 V} (\Delta_R S_A - \Delta_R S_B)^2 \Delta T^2 \frac{\left(\frac{dQ_A}{dE_A}\right) \left(\frac{dQ_B}{dE_B}\right)}{\left(\frac{dQ_B}{dE_B} + \frac{dQ_A}{dE_A}\right)} \quad (1)$$

Theoretical prediction of the energy gain according to eqn (1) requires knowledge of the reaction entropies and differential capacities of the electrode materials, which were determined by electrochemical measurements. From Fig. 2b and c can be seen that the entropies of Li intercalation in LCO and NCM and the differential capacities show a clear dependence on Li concentration in the materials. Note that for the sake of comparability, these data are plotted as a function of the chemical potential of Li ( $\mu_{\text{Li}}$ ), because the thermo-electrical energy conversion requires similar electrode potentials in the initial state. The changes in material-specific properties as a function of Li concentration correlate with phase diagrams, as demonstrated by the pioneering work of Delmas since the early 1980s.<sup>16,17</sup> For example, for  $0.95 < x < 0.75$  in  $\text{Li}_x\text{CoO}_2$ , a two-phase region exists between a Li-rich and a Li-poor phase.<sup>18</sup> Due to the differences in configurational as well as electronic entropy between these two phases, the reaction entropy in the two-phase region is relatively high (cf.  $\Delta_R S$  peak of LCO at  $\mu_{\text{Li}} = 3.9$  eV). For first order phase transitions, the chemical potential is constant (non-Nernstian behaviour),<sup>19</sup> which results in high differential capacity (cf.  $dQ/dE$  peak of LCO at  $\mu_{\text{Li}} = 3.9$  eV). This behaviour is similar to pyroelectrics, positioned at the brink of a ferroelectric-to-paraelectric phase-transition (Curie temperature), where the second order derivatives of the free energy diverge. We want to emphasize that this property of topotactic solid-state reactions is a great advantage compared to reactions in solution, e.g. as present in typical thermocells, which are limited by the concentration dependence of the potential obeying the Nernst equation. Based on these data, the thermal-electrical energy conversion properties are estimated. The change in open-circuit voltage predicted from the entropies of Li-intercalation in LCO and NCM for a temperature change of 40 K are slightly higher than determined experimentally but reflects the  $\mu_{\text{Li}}$ -dependence very well (Fig. 2d). Similarly, the predicted electric charge transferred during discharging to 0 V corresponds to the experimental  $\mu_{\text{Li}}$ -dependence but is somewhat smaller than determined experimentally (Fig. 2e). This could be related to kinetic limitations that are not considered in our model. Accordingly, deviations also exist with respect to the energy gained per temperature cycle (Fig. 2f). Apart from small deviations in the absolute values, the comparison between theoretical predictions and experimental results clearly shows that our model is valid. Accordingly, optimization

potentials can be estimated and promising research directions can be identified.

In summary, we proposed a novel type of electrochemical cell for low-grade thermal energy harvesting that combines the advantages of pyroelectrics and thermocells. The proof-of-concept device uses the difference in entropy of Li-ion intercalation in LCO and NCM to convert temperature fluctuations directly into electricity. Based on the proposed working principle, the efficiency and power output of thermal to electrical energy conversion can be maximized by finding material combinations that (i) have similar electrochemical potential of the guest species, (ii) exhibit large differences in the reaction entropy and (iii) undergo first order phase transitions to have high differential capacity. The ability to use temperature changes opens advantageous options for the design and setup of devices used in situations where spatial temperature gradients are difficult to establish. Bulky heat sinks can be eliminated, and the design of larger devices with bipolar stacking would allow high voltages to be generated with relatively small temperature changes.

This work was funded by the Deutsche Forschungsgemeinschaft (DFG, German Research Foundation) – Project-ID 431628538.

## Conflicts of interest

There are no conflicts to declare.

## References

- 1 K. Biswas, J. He, I. D. Blum, C.-I. Wu, T. P. Hogan, D. N. Seidman, V. P. Dravid and M. G. Kanatzidis, *Nature*, 2012, **489**, 414.
- 2 E. Garofalo, M. Bevione, L. Cecchini, F. Mattiussi and A. Chiolerio, *Energy Technol.*, 2020, **8**, 2000413.
- 3 A. Nozariasbmarz, H. Collins, K. Souza, M. H. Polash, M. Hosseini, M. Hyland, J. Liu, A. Malhotra, F. M. Ortiz, F. Mohaddes, V. P. Ramesh, Y. Sargolzaeiaval, N. Snouwaert, M. C. Öztürk and D. Vashaee, *Appl. Energy*, 2020, **258**, 114069.
- 4 A. R. M. Siddique, S. Mahmud and B. van Heyst, *Renewable Sustainable Energy Rev.*, 2017, **73**, 730–744.
- 5 C. B. Vining, *Nat. Mater.*, 2009, **8**, 83.
- 6 M. F. Dupont, D. R. MacFarlane and J. M. Pringle, *Chem. Commun.*, 2017, **53**, 6288–6302.
- 7 D. Lingam, A. R. Parikh, J. Huang, A. Jain and M. Minary-Jolandan, *Int. J. Smart Nano Mater.*, 2013, **4**, 229–245.
- 8 S. Pandya, G. Velarde, L. Zhang, J. D. Wilbur, A. Smith, B. Hanrahan, C. Dames and L. W. Martin, *NPG Asia Mater.*, 2019, **11**, 26.
- 9 C. R. Bowen, J. Taylor, E. LeBoulbar, D. Zabek, A. Chauhan and R. Vaish, *Energy Environ. Sci.*, 2014, **7**, 3836–3856.
- 10 G. Sebald, D. Guyomar and A. Agbossou, *Smart Mater. Struct.*, 2009, **18**, 125006.
- 11 C. Heubner, T. Lein, M. Schneider and A. Michaelis, *J. Mater. Chem. A*, 2020, **8**, 16854–16883.
- 12 S. Laubach, S. Laubach, P. C. Schmidt, D. Ensling, S. Schmid, W. Jaegermann, A. Thissen, K. Nikolowski and H. Ehrenberg, *Phys. Chem. Chem. Phys.*, 2009, **11**, 3278.
- 13 Y. Koyama, I. Tanaka, H. Adachi, Y. Makimura and T. Ohzuku, *J. Power Sources*, 2003, **119–121**, 644–648.
- 14 A. Nickol, T. Schied, C. Heubner, M. Schneider, A. Michaelis, M. Bobeth and G. Cuniberti, *J. Electrochem. Soc.*, 2020, **167**, 90546.
- 15 R. B. Olsen, D. A. Bruno and J. M. Briscoe, *J. Appl. Phys.*, 1985, **58**, 4709–4716.
- 16 R. Berthelot, D. Carlier and C. Delmas, *Nat. Mater.*, 2011, **10**, 74–80.
- 17 L. Vitoux, M. Guignard, M. R. Suchomel, J. C. Pramudita, N. Sharma and C. Delmas, *Chem. Mater.*, 2017, **29**, 7243–7254.
- 18 A. van der Ven, M. K. Aydinol, G. Ceder, G. Kresse and J. Hafner, *Phys. Rev. B: Condens. Matter Mater. Phys.*, 1998, **58**, 2975.
- 19 G. Ceder and A. Van der Ven, *Electrochim. Acta*, 1999, **45**, 131–150.

